Radiotherapy and Oncology 137 (2019) 125–129

Contents lists available at ScienceDirect

Radiotherapy and Oncology

journal homepage: www.thegreenjournal.com

Short Communication

In vitro biological response of cancer and normal tissue cells to proton irradiation not affected by an added magnetic field

Peter W. Nagle [a,b,c], Marc-Jan van Goethem [b,d], Marco Kempers [a], Harry Kiewit [d], Antje Knopf [b], Johannes A. Langendijk [b], Sytze Brandenburg [d], Peter van Luijk [a,b], Rob P. Coppes [a,b,*]

[a] *Department of Biomedical Sciences of Cells and Systems, Section Molecular Cell Biology;* [b] *Department of Radiation Oncology;* [c] *Department of Surgical Oncology, University Medical Center Groningen; and* [d] *KVI Center for Advanced Radiation Technology, University of Groningen, The Netherlands*

ARTICLE INFO

Article history:
Received 21 March 2019
Received in revised form 19 April 2019
Accepted 23 April 2019
Available online 11 May 2019

Keywords:
Protons
MRI
Tumor
Normal tissue
Organoids

ABSTRACT

To optimize beam delivery and conformality of proton therapy, MRI integration has been proposed. Therefore, we investigated if proton irradiation in a magnetic field would change biological responses. Our data in cancer cell lines and stem cell-derived organoid models suggest that a magnetic field does not modify the biological response.

The primary objective of radiotherapy as a cancer treatment is to eradicate tumor cells while minimizing the effects to surrounding healthy tissues [1]. Due to their physical nature, particles, such as protons, can be used for more conformal dose delivery to the tumor than photon-based conventional irradiation techniques, thus more effectively sparing normal tissue from unnecessary doses [2–5]. Real-time imaging during proton therapy could further optimize the delivery of the beam to patients and offer even more accurate normal tissue sparing [6]. The good soft-tissue contrast of magnetic resonance imaging (MRI) in radiotherapy is very useful. Indeed, MRI has been successfully integrated into photon-based radiotherapy devices [7–9]. However, integration of MRI into proton radiotherapy changes various aspects of dose delivery.

It has been shown that the application of a magnetic field to a proton beam can both decrease the depth of the Bragg peak and laterally shift the beam [10]. This shift can be accurately predicted [10] and therefore compensated for. However, although MRI has been successfully integrated into IMRT devices [9], the biological effects of an added magnetic field during proton irradiation have not yet been investigated. Therefore, the aim of this study was to determine if proton irradiation in a magnetic field would induce differential biological outcomes to proton irradiation alone. Our results suggest that biological responses to MR-guided proton therapy will be similar to that of conventional proton therapy.

Materials and methods

Proton irradiations

The cells were irradiated with protons in the center of a homogeneous magnetic field which was switched between 0 (off) and 1.01 T (on). The magnetic field was directed horizontally at 90 degrees with respect to the beam direction. For the irradiations a 150 MeV proton beam was produced by the AGOR cyclotron of the University of Groningen. The irradiation field was created by scattering the 150 MeV proton beam using a 1.44 mm lead scatter foil at 3.5 m in front of the samples. The field size was defined by a 30 mm collimator outside the magnetic field at 57 cm from the samples. At the position of the sample the proton beam energy was 130 MeV (LET = 0.6 keV/μm) due to energy losses in the scatter foil, air, beam intensity monitor and 2 cm polyethylene build-up material directly in front of the samples. This is in the plateau region of the 150 MeV Bragg curve. The field homogeneity was measured using a LANEX scintillation screen at the sample position using a CCD camera as described by [11] with the magnet on and off. The ratio of light output with magnet on and magnet off was 0.998 ± 0.0019. Therefore, no significant difference in light output was observed suggesting that the magnetic field does not influence dose. The magnetic field bends the beam, shifting the vertical posi-

* Corresponding author at: Department of Biomedical Sciences of Cells and Systems, Section Molecular Cell Biology, University Medical Center Groningen, University of Groningen: Ant. Deusinglaan 1, 9713 AV Groningen, The Netherlands.
E-mail address: r.p.coppes@umcg.nl (R.P. Coppes).

https://doi.org/10.1016/j.radonc.2019.04.028
0167-8140/

tion of the irradiation field by 6.4 mm at sample position. The vertical position of the samples irradiated with the magnetic field on was adjusted such that the samples stayed centered in the irradiation field. In both cases the homogeneity of the field was 2% over the inner 28 mm diameter. As the samples are 26 mm in diameter, every other well was used in the 12-well plates in order to avoid overlap of successive radiation fields. The applied dose was controlled using a large-diameter ionization chamber 2 m upstream of the samples. The ionization chamber was calibrated against a calibrated Markus chamber following the protocol described in chapter 10 of TRS-398 [12]. The calibration procedure was performed both with the magnet on and off, no significant difference was observed between the two calibration measurements. The ratio of the calibration factors for magnet on divided by magnet off was 1.0006 ± 0.0009.

Cell line culturing and clonogenic survival assays

Human embryonic kidney (HEK293) and human lung adenocarcinoma (A549) cell lines were cultured in Dulbecco's Modified Eagle medium (DMEM) (Gibco, Life Technologies) supplemented with 10% fetal calf serum and 1% Penicillin/Streptomycin. Cells were maintained at 37 °C, 5% CO_2.

Clonogenic survival assays were performed similar to methods described in [13,14]. All irradiations were performed on 70–80% confluent cells in sealed 12-well plates, described in [15]. Following irradiation, cells were detached from the plates by incubating for 5 min with trypsin/0.05% EDTA (Gibco). Cells were counted and seeded in triplicate in 6-cm dishes at dose-dependent concentrations. After 10–14 days colonies were fixed and stained by incubating with 0.1% (w/v) Coomassie Brilliant Blue, 50% methanol, and 10% acetic acid for 30–60 min and colonies containing ≥50 cells were counted. All experiments were normalized for plating efficiency of control (0 Gy).

Immunofluorescent staining

Two days prior to irradiation, cells were seeded in glass-bottomed 12-well tissue culture plates (In Vitro Scientific, p12-1.5H-N). At specified time points post-irradiation, cells were fixed for 15 min in 2% paraformaldehyde and permeabilized in 0.2% Triton X-100 for 10 min.

All samples were incubated overnight at 4 °C with anti-53BP1 primary antibody (H-300) (1:500; Santa Cruz, sc-22760, rabbit), followed by incubation at room temperature with an Alexa Fluor 594 secondary antibody (1:800; Life technologies, A110012, goat anti-rabbit)) for 90 min. Nuclear staining was performed using Hoechst-33342 (Molecular Probes, Life Technologies). Imaging was performed using TissueFAxs (Tissuegnostics).

Mouse salivary gland stem cell isolation and culturing

Salivary glands were dissected from 8-12 week old female C57BL/6 mice (Harlan, The Netherlands). SG cells were isolated and cultured to form spheres as described previously [16–19]. In short, salivary glands were mechanically disrupted, followed by enzymatic digestion using digestion enzymes collagenase type II (Gibco) and hyaluronidase (Sigma Aldrich). After filtering, cells were seeded into 12-well plates in DMEM-F12 medium (Gibco) containing 1% penicillin/streptomycin (Gibco), glutamax (2 mM, Gibco), epidermal growth factor (20 ng/ml, Sigma Aldrich), fibroblast growth factor-2 (20 ng/ml, Peprotech), 1% N2 supplement (Gibco), insulin (10 μg/ml, Sigma) and dexamethasone (1 μM, Sigma). After three days, primary spheres (passage 0) were disrupted using 0.05% trypsin-EDTA (Gibco) into single cells and reseeded at 1×10^4 cells/well in Matrigel and medium supplemented with ROCK1-inhibitor (Y-27632 (Sigma-Aldrich)) was added to the gels (passage 1).

Mouse salivary gland stem cell survival assay

To determine the sensitivity of mouse salivary gland stem cells (SGSCs), a modified 3D-survival assay was performed as described in [14]. Single cells were seeded in Matrigel, as described above, 2 h pre-irradiation with 0–6 Gy. Mouse SGSCs were plated at a density of 1×10^4 cells per well (0–2 Gy) or 2×10^4 cells per well (4–6 Gy). One-week post-irradiation, spheres and cells were counted. Survival was calculated as follows:

$$\textit{Sphere forming potential} = \frac{\text{Number of spheres harvested}}{\text{Cells seeded}} \times 100$$

$$\textit{Surviving fraction} = \frac{\text{Sphere forming potential treated}}{\text{Sphere forming potential at 0 Gy}}$$

Statistical analysis

All values presented as the mean ± standard error of the mean of ≥3 independent experiments. Statistical significance was tested by *t*-test analysis using GraphPad Prism (GraphPad software). Power analysis was performed and is provided in the supplementary document.

Results

To determine if adding a magnetic field to proton irradiation induced a differential effect in cellular survival, clonogenic assays [20] were performed on two cancerous cell lines, A549 and HEK293. In both cell lines, no differences were observed in terms of survival following proton irradiation with or without a magnetic field (Fig. 1A and B). These results suggest that a magnetic field does not change the response of these cancer cell lines to proton irradiation.

While the addition of a magnetic field during irradiation had no effect on survival, it could still have an effect on other important biological outcomes. Therefore, we investigated whether the addition of a magnetic field during irradiation resulted in a differential response in DNA damage induction and repair. To this end we used U2OS cells, which are specifically suitable for DNA damage immunofluorescent staining [21,22]. These cells were irradiated with protons within a magnetic field or irradiated with protons alone. Thirty min after irradiation, 53BP1 was assessed as a marker for DNA double stranded breaks [21,23] by immunofluorescent staining (Fig. 1C). There was no significant difference in terms of number of foci induced following proton irradiation in or outside the magnetic field (Fig. 1D). Furthermore, in both cases all cells were found to be positive for induced damage (4 or more foci) following irradiation (Fig. S1).

While there were no observed differences in the levels of DNA damage induced following proton irradiation in a magnetic field compared to proton irradiation alone, proton irradiation within a magnetic field could potentially induce a more complex DNA damage which could be repaired differently than damage caused by proton irradiation alone. Therefore, 53BP1 levels were further determined at 4 and 24 hours after irradiation (Fig. 1C). 53BP1 foci were found to be reduced in cells irradiated inside and outside a magnetic field at both 4 hours and 24 hours (Fig. 1E). However, no significant differences were observed in the number of foci at both time points following irradiation (Fig. 1E). Also, no differences in the percentage of cells found to be positive for induced DNA damage 4 hours and 24 hours post-irradiation (Fig. S1) were

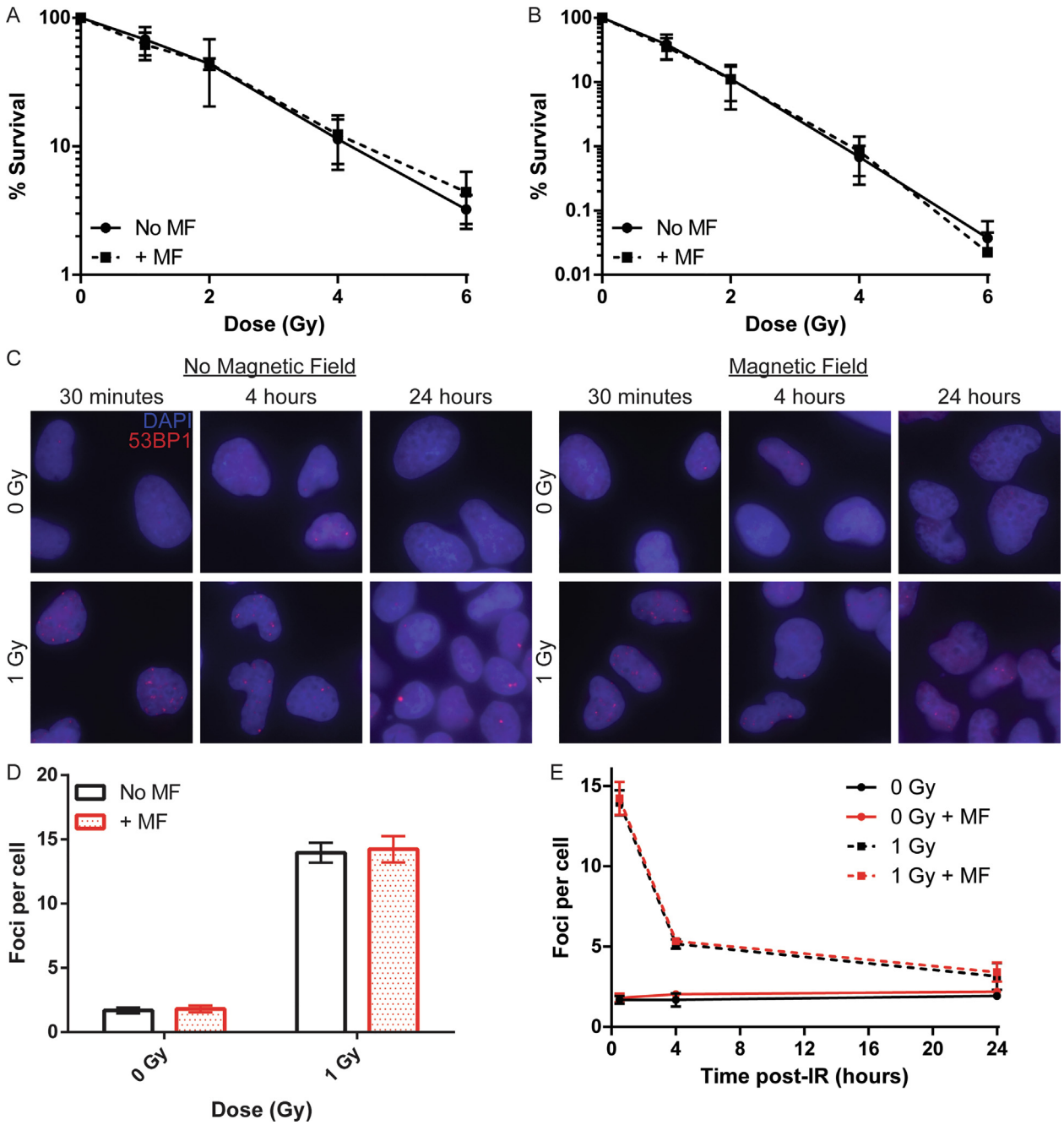

Fig. 1. Proton irradiation within a magnetic field does not affect the survival or DNA damage repair of cell lines compared to proton irradiation alone. Clonogenic survival of (A) A549 and (B) HEK293 cells in response to proton irradiation with (+MF) or without (No MF) a magnetic field. $N = 4$, error bars represent SD. (C) Representative images of 53BP1 (red) foci in proton irradiated U2OS cells in the presence or absence of a magnetic field (nuclei are counter-stained with Hoechst). (D) Quantification of the 53BP1 induced in U2OS cells 30 min post-irradiation within a magnetic field. (E) Kinetic clearance of 53BP1 foci following proton irradiation within a magnetic field or without a magnetic field. $N = 3$, error bars represent SD.

observed. These results indicate that proton irradiation within a magnetic field doesn't affect either the induction or clearance of DNA double stranded breaks in cancerous cell lines compared to proton irradiation alone.

To investigate if normal tissue was differentially affected by proton irradiation alone than by proton irradiation within a magnetic field, we irradiated mouse salivary gland stem cells with protons and assessed the development of secondary organoids as a readout for survival compared to non-irradiated cells (Fig. 2) [14,24]. Whether or not the cells were irradiated within a magnetic field had no influence in the outcome of the survival, with increasing doses resulting in decreased organoid forming efficiency in both conditions (Fig. 2B).

Taken together these results indicate that adding a magnetic field to proton irradiation does not modify the biological response to irradiation.

Discussion

The optimization of radiotherapy as a cancer treatment involves delivering an adequate dose to the tumor, while minimizing the

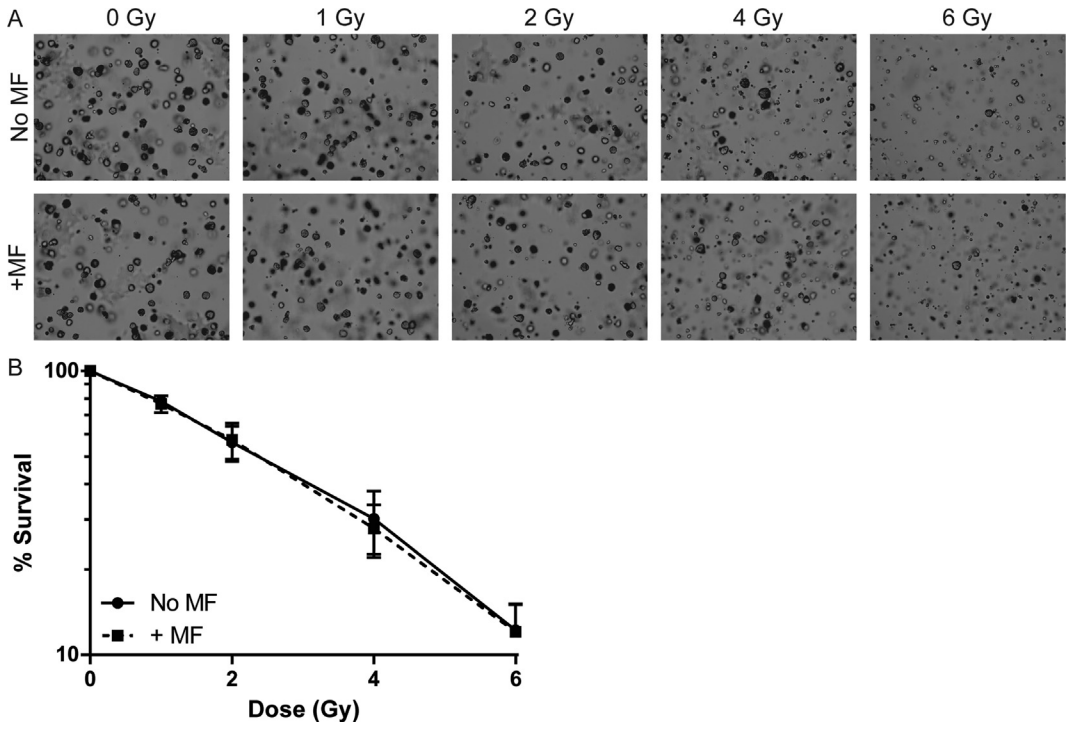

Fig. 2. Normal tissue stem cells are not differentially affected by proton irradiations within a magnetic compared to proton irradiation alone. (A) Representative images of mouse salivary gland stem cell organoids 1 week after proton irradiation as single cells without a magnetic field (No MF) or within a magnetic field (+MF) (0–2 Gy were seeded at 10,000 cells per well, while 4 and 6 Gy were seeded at 20,000 cells per well). (B) Quantification of the clonogenic survival of mouse salivary gland stem cells in response to proton irradiation with or without a magnetic field present. $N = 6$, error bars represent SD.

dose (and thus side effects) to normal tissues surrounding the tumor. The use of protons for irradiation allows for a better dose conformity to the target volume than conventional photon-based treatment modalities [5]. However, the use of proton therapy still results in unwanted dose to healthy surrounding tissue which may lead to complications. Advanced imaging techniques allow for the tumor to be visualized in real-time during irradiation and may therefore facilitate more accurate dose delivery. Therefore, combining real-time MRI with IMRT to enhance the healthy tissue sparing during radiation was already suggested long ago [25]. In vitro studies showed that an additional magnetic field during photon irradiation had little to no effect on viability of a panel of tumor cell lines [26]. However, there were concerns about the effects of a magnetic field on electrons at the tissue-surface interface, as this may enhance the local dose at the tissue surface [8,27,28]. Nonetheless, MRI with a 1.5 T magnetic field has been successfully integrated into a linear accelerator used for photon-based treatments. This resulted in highly accurate dose delivery [8,9] and shows promise for the idea of MRI-guided radiotherapy treatment. Therefore, integrating MRI into proton therapy facilities has been proposed to further increase the accuracy of treatment, and thus spare more healthy tissue [6,29].

However, the differential effects on biological outcomes of adding a magnetic field to protons have not been assessed. Therefore, the aim of this paper was to assess the biological effects of magnetic field integration during proton irradiation. Introduction of a magnetic field during proton irradiation didn't change survival in cancer-derived HEK293 or A549 cell lines, similar to the effects of an added magnetic field during photon irradiation [26], nor did it affect the induction and clearance of DNA damage in cell lines. Also, the survival of normal tissue stem cells, as measured by an organoid forming survival assay [14,24], was not affected by a magnetic field during proton irradiation.

Normal tissue side effects cause a dramatic reduction in the quality of life of patients following irradiation as part of a cancer treatment [30,31]. Sparing important organs, or even specific parts of an organ, can have a significant impact in reducing normal tissue side effects [32]. Our results show that important biological outcomes (survival and DNA damage repair) following proton irradiation are not differentially affected by the addition of a magnetic field. Therefore, given the potential benefit of live imaging during treatments, the development of MR-proton irradiation facilities could be a promising future direction to improve radiotherapy as important regions of tissue could potentially be better spared [32].

Conflict of interest

The authors declare no conflicts of interests.

Appendix A. Supplementary data

Supplementary data to this article can be found online at https://doi.org/10.1016/j.radonc.2019.04.028.

References

[1] Thariat J, Hannoun-Levi JM, Sun Myint A, Vuong T, Gerard JP. Past, present, and future of radiotherapy for the benefit of patients. Nat Rev Clin Oncol 2013;10:52–60.
[2] Durante M, Orecchia R, Loeffler JS. Charged-particle therapy in cancer: clinical uses and future perspectives. Nat Rev Clin Oncol 2017.
[3] Lomax AJ. Charged particle therapy: the physics of interaction. Cancer J 2009;15:285–91.
[4] Newhauser WD, Zhang R. The physics of proton therapy. Phys Med Biol 2015;60:R155–209.
[5] Mitin T, Zietman AL. Promise and pitfalls of heavy-particle therapy. J Clin Oncol 2014;32:2855–63.
[6] Oborn BM, Dowdell S, Metcalfe PE, Crozier S, Mohan R, Keall PJ. Future of medical physics: real-time MRI-guided proton therapy. Med Phys 2017;44:e77–90.
[7] Lagendijk JJ, Raaymakers BW, Van den Berg CA, Moerland MA, Philippens ME, van Vulpen M. MR guidance in radiotherapy. Phys Med Biol 2014;59:R349–69.

[8] Lagendijk JJ, Raaymakers BW, van Vulpen M. The magnetic resonance imaging-linac system. Semin Radiat Oncol 2014;24:207–9.
[9] Raaymakers BW, Jurgenliemk-Schulz IM, Bol GH, Glitzner M, Kotte ANTJ, van Asselen B, et al. First patients treated with a 1.5 T MRI-linac: clinical proof of concept of a high-precision, high-field MRI guided radiotherapy treatment. Phys Med Biol 2017;62:L41–50.
[10] Schellhammer SM, Gantz S, Luhr A, Oborn BM, Bussmann M, Hoffmann AL. Technical note: experimental verification of magnetic field-induced beam deflection and bragg peak displacement for MR-integrated proton therapy. Med Phys. 2018;45:3429–34.
[11] Boon SN, van Luijk P, Schippers JM, Meertens H, Denis JM, Vynckier S, et al. Fast 2D phantom dosimetry for scanning proton beams. Med Phys. 1998;25:464–75.
[12] International Atomic Energy Agency. Absorbed dose determination in external beam radiotherapy: an international code of practice for dosimetry based on standards of absorbed dose to water (v.12). Vienna: International Atomic Energy Agency; 2006.
[13] Chiu RK, Brun J, Ramaekers C, Theys J, Weng L, Lambin P, et al. Lysine 63-polyubiquitination guards against translesion synthesis-induced mutations. PLoS Genet 2006;2:e116.
[14] Nagle PW, Hosper NA, Ploeg EM, van Goethem MJ, Brandenburg S, Langendijk JA, et al. The in vitro response of tissue stem cells to irradiation with different linear energy transfers. Int J Radiat Oncol Biol Phys 2016;95:103–11.
[15] Niemantsverdriet M, van Goethem MJ, Bron R, Hogewerf W, Brandenburg S, Langendijk JA, et al. High and low LET radiation differentially induce normal tissue damage signals. Int J Radiat Oncol Biol Phys 2012;83:1291–7.
[16] Lombaert IM, Brunsting JF, Wierenga PK, Faber H, Stokman MA, Kok T, et al. Rescue of salivary gland function after stem cell transplantation in irradiated glands. PLoS One 2008;3:e2063.
[17] Pringle S, Nanduri LS, van der Zwaag M, van Os R, Coppes RP. Isolation of mouse salivary gland stem cells. J Vis Exp 2011. pii: 2484. doi:10.3791/2484.
[18] Nanduri LS, Baanstra M, Faber H, Rocchi C, Zwart E, de G, Haan, et al. Purification and ex vivo expansion of fully functional salivary gland stem cells. Stem Cell Rep 2014;3:957–64.
[19] Maimets M, Rocchi C, Bron R, Pringle S, Kuipers J, Giepmans BN, et al. Long-term in vitro expansion of salivary gland stem cells driven by wnt signals. Stem Cell Rep 2016;6:150–62.
[20] Franken NA, Rodermond HM, Stap J, Haveman J, van Bree C. Clonogenic assay of cells in vitro. Nat Protoc 2006;1:2315–9.
[21] Schultz LB, Chehab NH, Malikzay A, Halazonetis TD. p53 binding protein 1 (53BP1) is an early participant in the cellular response to DNA double-strand breaks. J Cell Biol 2000;151:1381–90.
[22] Sollazzo A, Brzozowska B, Cheng L, Lundholm L, Scherthan H, Wojcik A. Live dynamics of 53BP1 foci following simultaneous induction of clustered and dispersed DNA damage in U2OS cells. Int J Mol Sci 2018;19. https://doi.org/10.3390/ijms19020519.
[23] Gupta A, Hunt CR, Chakraborty S, Pandita RK, Yordy J, Ramnarain DB, et al. Role of 53BP1 in the regulation of DNA double-strand break repair pathway choice. Radiat Res 2014;181:1–8.
[24] Nagle PW, Hosper NA, Barazzuol L, Jellema AL, Baanstra M, van Goethem MJ, et al. Lack of DNA damage response at low radiation doses in adult stem cells contributes to organ dysfunction. Clin Cancer Res 2018.
[25] Lagendijk JJ, Raaymakers BW, Raaijmakers AJ, Overweg J, Brown KJ, Kerkhof EM, et al. MRI/linac integration. Radiother Oncol 2008;86:25–9.
[26] Wang L, Hoogcarspel SJ, Wen Z, van Vulpen M, Molkentine DP, Kok J, et al. Biological responses of human solid tumor cells to X-ray irradiation within a 1.5-tesla magnetic field generated by a magnetic resonance imaging-linear accelerator. Bioelectromagnetics 2016;37:471–80.
[27] Raaijmakers AJ, Hardemark B, Raaymakers BW, Raaijmakers CP, Lagendijk JJ. Dose optimization for the MRI-accelerator: IMRT in the presence of a magnetic field. Phys Med Biol. 2007;52:7045–54.
[28] Chen X, Prior P, Chen GP, Schultz CJ, Li XA. Technical note: dose effects of 1.5 T transverse magnetic field on tissue interfaces in MRI-guided radiotherapy. Med Phys 2016;43:4797.
[29] Moteabbed M, Schuemann J, Paganetti H. Dosimetric feasibility of real-time MRI-guided proton therapy. Med Phys 2014;41:111713.
[30] Bijl HP, van Luijk P, Coppes RP, Schippers JM, Konings AW, van Der Kogel AJ. Regional differences in radiosensitivity across the rat cervical spinal cord. Int J Radiat Oncol Biol Phys 2005;61:543–51.
[31] Jellema AP, Slotman BJ, Doornaert P, Leemans CR, Langendijk JA. Impact of radiation-induced xerostomia on quality of life after primary radiotherapy among patients with head and neck cancer. Int J Radiat Oncol Biol Phys 2007;69:751–60.
[32] van Luijk P, Pringle S, Deasy JO, Moiseenko VV, Faber H, Hovan A, et al. Sparing the region of the salivary gland containing stem cells preserves saliva production after radiotherapy for head and neck cancer. Sci Transl Med 2015;7:305ra147.